

PAPER

Iterative Algorithm for Reducing the Peak-to-Average Power Ratio of Feedback-Controlled Multitone-Hopping CDMA Signals

Kazuki CHIBA^{†a)}, *Student Member* and Masanori HAMAMURA[†], *Member*

SUMMARY A novel peak-to-average power ratio (PAR) control algorithm for feedback-controlled multitone-hopping code-division multiple access (FC/MH-CDMA) signals is proposed. In FC/MH-CDMA, since each chip consists of plural tones, the energy consumption due to a large PAR is not negligible at the transmitter. The proposed PAR control algorithm iteratively constructs a time-frequency code that achieves a preset, target PAR under the condition that all signals are asynchronously transmitted. A PAR of 1 dB is shown to be achievable, and the bit-error rate performance is shown to be only slightly influenced if the target PAR is set to be larger than 3 dB. The influence of quantization is also discussed in terms of its application to limited feedback channels.

key words: CDMA, asynchronous, multipath, feedback, multitone, PAR

1. Introduction

Intersymbol interference (ISI) and multiple access interference (MAI) are two primary causes of the deterioration of wireless communication performance [1]–[4]. Feedback-based systems have been investigated in an attempt to greatly reduce ISI and MAI [5]. For uplink channels, a method in which a base station (BS) uses an adaptive filter at a receiver to produce an analog pseudo-noise (PN) sequence, which is assigned to a new user, was proposed [6] in the context of direct-sequence code-division multiple access (DS-CDMA). Analog PN sequences can be orthogonal to each other under arbitrary asynchronous conditions. For synchronous DS-CDMA, an iterative construction method that produces signature sequences using a minimum mean-squared error (MMSE) filter was proposed [7]. This method was demonstrated to produce a set of Welch bound equality (WBE) sequences [8], [9] using an MMSE filter, the size of which is identical to the length of the signature sequence. In contrast, we previously proposed feedback-controlled DS-CDMA (FC/DS-CDMA) [10], in which the receiver uses an adaptive filter that is larger than the length of the signature sequence and returns part of the filter coefficients to the transmitter. This method has been shown to have superior performance in terms of bit-error rate (BER) over time-invariant multipath channels. Furthermore, we proposed feedback-controlled multitone-hopping CDMA (FC/MH-CDMA), which combines frequency-hopping CDMA (FH-CDMA) with FC/DS-CDMA, to increase the signal-to-interference plus noise ra-

tio (SINR) [11]. Each receiver of FC/MH-CDMA is composed of a time-frequency, two-dimensional, adaptive finite-duration impulse response (FIR) filter, which is larger than the hopping pattern. The receiver returns part of the filter coefficients to the transmitter. The signals transmitted in FC/MH-CDMA consist of coded multiple-frequency tones.

In order to address the large peak-to-average power ratio (PAR) of multicarrier signals, which results in increased energy consumption at the transmitter, PAR reduction techniques have been discussed. Clipping is one of the easiest PAR reduction methods [12]. When the amplitude of multicarrier signals exceeds the threshold, clipping replaces the amplitude with the threshold level. In the selected mapping [13], the transmitter generates plural multicarrier signals that have the same message symbols with independent phase rotation, and the transmitter selects a signal that minimizes the PAR in the plural multicarrier signals. Using block codes, the PAR of multicarrier signals can be reduced [14], [15]. For example, the multicarrier signals using Golay complementary sequences limit the value of the PAR at 3 dB. Recently, on the other hand, DS-CDMA has also been reconsidered for the applications of synchronous or quasi-synchronous uplink channels [16] because of its small PAR [17]*.

Typically, since the performance, such as the BER and/or user capacity, of multicarrier signals is deteriorated by such a PAR reduction technique, it is of extreme importance for FC/MH-CDMA to find a PAR reduction technique that has minimal impact on the BER and user capacity, even for asynchronous multiple access. Previously, we investigated the PAR of FC/MH-CDMA signals and showed that several techniques, such as tone selection by limiting the number of tones per chip, quantization for reducing the overhead for feedback, and clipping the time-frequency code, are effective for reducing the PAR by a few dB at an almost identical BER [18].

In this paper, we propose a PAR reduction algorithm

*The block transmission of DS-CDMA enables us to shorten the relative duration of the cyclically prefixed (and/or postfixed) guard interval (CP-GI), which reduces the losses of required energy and transmission rate. The techniques of two-dimensional spreading and MMSE frequency-domain equalization (MMSE-FDE) effectively suppress ISI and MAI, and offer a significant improvement in BER over synchronous or quasi-synchronous uplink channels [16]. FC/MH-CDMA does not require such an extra guard interval and is applicable to asynchronous uplink or decentralized multiple-access systems [11].

Manuscript received September 14, 2009.

Manuscript revised March 26, 2010.

[†]The authors are with the Graduate School of Engineering, Kochi University of Technology, Kami-shi, 782-8502 Japan.

a) E-mail: chiba@m.ieice.org

DOI: 10.1587/transcom.E93.B.3072

for FC/MH-CDMA signals, which controls the PAR to a preset target value with good BER performance over asynchronous and time-invariant multipath channels.

The remainder of this paper is organized as follows. FC/MH-CDMA is introduced in Sect. 2. In Sect. 3, an iterative PAR control algorithm for reducing the PAR of FC/MH-CDMA signals is presented. The effectiveness of the proposed algorithm is verified in Sect. 4.

2. FC/MH-CDMA

2.1 Transmitter

We assume the uplink multiple access shown in Fig. 1. A signal received at the position of BS can be modeled as the sum of K signals that are independently transmitted through distinct channels. The transmitter and receiver for the k th signal ($k = 1, 2, \dots, K$) of FC/MH-CDMA are shown in Fig. 2.

The signature waveform $c_k(t)$ for the k th signal is given by

$$c_k(t) = \sum_{l=1}^L a_{k,l}(t - (l-1)T_c), \quad (1)$$

where $a_{k,l}(t)$ ($0 < t < T_c$; T_c [s] is the chip duration) is the l th chip waveform ($l = 1, 2, \dots, L$; L is the number of chips) for $c_k(t)$, which is given by

$$a_{k,l}(t) = g(t) \sum_{m=1}^M p_{k,l,m} e^{j2\pi \frac{m-1}{T_c} t}, \quad (2)$$

where $j = \sqrt{-1}$, $p_{k,l,m}$ is the complex amplitude of the m th tone of frequency $\frac{m-1}{T_c}$ [Hz] ($m = 1, 2, \dots, M$; M is the number of transmittable tones per chip) for the l th chip of $c_k(t)$, and $g(t) = \{1(0 < t < T_c), 0(\text{otherwise})\}$.

Let \mathbf{P}_k be an $L \times M$ matrix that contains $p_{k,l,m}$ such that

$$\mathbf{P}_k = \begin{bmatrix} p_{k,1,1} & p_{k,1,2} & \cdots & p_{k,1,M} \\ p_{k,2,1} & p_{k,2,2} & \cdots & p_{k,2,M} \\ \vdots & \vdots & \ddots & \vdots \\ p_{k,L,1} & p_{k,L,2} & \cdots & p_{k,L,M} \end{bmatrix}. \quad (3)$$

The matrix \mathbf{P}_k is referred to as the hopping pattern or time-frequency code for the k th signal.

The k th signal transmitted by the transmitter is given

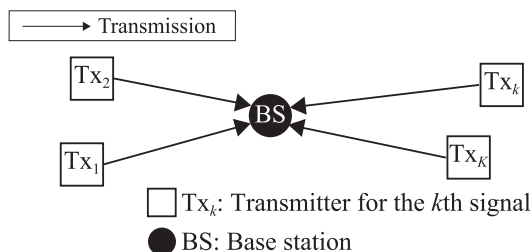


Fig. 1 Uplink multiple access (asynchronous transmission).

by

$$s_k(t) = \sum_{n=0}^{\infty} b_k(n) c_k(t - nT_s), \quad (4)$$

where $b_k(n)$ is a complex message symbol transmitted in $nT_s < t < (n+1)T_s$ ($n = 0, 1, \dots$), and T_s [s] is the symbol duration ($T_s = LT_c$). In this paper, we assume that $b_k(n)$ is a quaternary phase-shift keying (QPSK) symbol.

2.2 Channel

Let $h_k(t)$ be the impulse response of the channel through which the k th signal ($k = 1, 2, \dots, K$) is transmitted to the BS, as given by

$$h_k(t) = \sum_{i=1}^{I_k} h_{k,i} \delta(t - \tau_{k,i}), \quad (5)$$

where $h_{k,i} (= |h_{k,i}| e^{j\theta_{k,i}})$ is the complex gain constant for the i th path of the channel, $\tau_{k,i}$ ($0 \leq \tau_{k,i} < T_s$) is the delay for the i th path, and I_k is the number of paths of the channel.

The received signal $r(t)$ at the position of the BS is given by

$$r(t) = \sum_{k=1}^K (s_k(t) * h_k(t)) + n(t) \quad (6)$$

$$= \sum_{k=1}^K \sum_{n=0}^{\infty} \sum_{i=1}^{I_k} h_{k,i} b_k(n) c_k(t - nT_s - \tau_{k,i}) + n(t), \quad (7)$$

where $n(t)$ is an additive white Gaussian noise (AWGN) with a double-sided power spectral density of $N_0/2$ [W/Hz].

2.3 Receiver

The receiver for the k th signal is composed of the adaptive FIR filter and operates symbol-by-symbol. The FIR filter has $(L + \alpha) \times M$ complex weights ($0 \leq \alpha \leq L$), which are used for recovering the message symbol $b_k(n)$ while reducing ISI and MAI. In FC/MH-CDMA, the receiver filter is larger than the hopping pattern \mathbf{P}_k , as shown in Fig. 2, to fully collect the received, time-spread energy over the multipath channel and to produce an updated hopping pattern that efficiently achieves a smaller BER [10], [11]. Let \mathbf{W}_k be an $(L + \alpha) \times M$ matrix, the (l, m) th entry of which is the complex weight $w_{k,l,m}$ of the receiver. The weight matrix \mathbf{W}_k is updated by an adaptive algorithm. In this paper, we adopt a normalized least-mean-square (N-LMS) algorithm [19], which is one of the less complex adaptation algorithms. For simplicity, the receiver for the k th signal is assumed to be synchronized with the first path of the channel $h_k(t)$. The k th receiver obtains discrete-time samples of every frequency and chip from the received signal $r_k(t)$. The m th frequency component $r_{k,l,m}$, detected at $t = nT_s + lT_c + \tau_{k,1}$ ($l = 1, 2, \dots, L + \alpha$), is given by

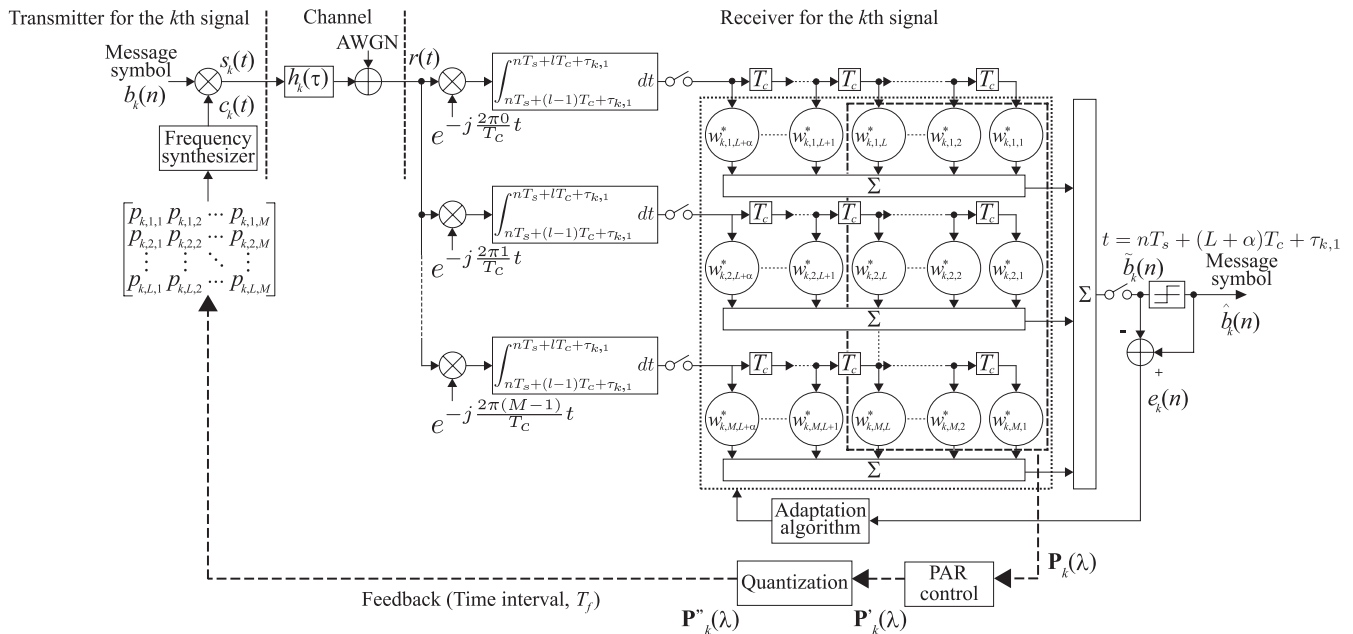


Fig. 2 Transmitter and receiver for the k th signal.

$$r_{k,l,m}(n) = \int_{nT_s+(l-1)T_c+\tau_{k,1}}^{nT_s+lT_c+\tau_{k,1}} r_k(t) e^{-j\frac{2\pi(m-1)}{T_c}t} dt. \quad (8)$$

We define the $(L + \alpha) \times M$ matrix $\mathbf{R}_k(n)$ that contains the samples detected in $nT_s + \tau_{k,1} < t < nT_s + (L + \alpha)T_c + \tau_{k,1}$ as

$$\mathbf{R}_k(n) = \begin{bmatrix} r_{k,1,1}(n) & r_{k,1,2}(n) & \cdots & r_{k,1,M}(n) \\ r_{k,2,1}(n) & r_{k,2,2}(n) & \cdots & r_{k,2,M}(n) \\ \vdots & \vdots & \ddots & \vdots \\ r_{k,L,1}(n) & r_{k,L,2}(n) & \cdots & r_{k,L,M}(n) \\ r_{k,1,1}(n+1) & r_{k,1,2}(n+1) & \cdots & r_{k,1,M}(n+1) \\ r_{k,2,1}(n+1) & r_{k,2,2}(n+1) & \cdots & r_{k,2,M}(n+1) \\ \vdots & \vdots & \ddots & \vdots \\ r_{k,\alpha,1}(n+1) & r_{k,\alpha,2}(n+1) & \cdots & r_{k,\alpha,M}(n+1) \end{bmatrix}. \quad (9)$$

The FIR filter output $\tilde{b}_k(n)$ can be represented as

$$\tilde{b}_k(n) = \text{tr}[\mathbf{W}_k^H(n)\mathbf{R}_k(n)], \quad (10)$$

where the superscript H denotes the complex conjugate and transpose of the matrix, and $\text{tr}[\cdot]$ denotes the trace of the matrix.

The weight matrix $\mathbf{W}_k(n)$ is updated as

$$\mathbf{W}_k(n+1) = \mathbf{W}_k(n) + \frac{\mu \mathbf{R}_k(n) e_k^*(n)}{\|\mathbf{R}_k(n)\|_F^2}, \quad (11)$$

where μ is the step size parameter, and $\|\mathbf{R}_k(n)\|_F$ denotes the Frobenius norm of the received signal matrix $\mathbf{R}_k(n)$, which is defined as

$$\|\mathbf{R}_k(n)\|_F = \sqrt{\sum_{l=1}^{L+\alpha} \sum_{m=1}^M |r_{k,l,m}(n)|^2}. \quad (12)$$

In addition, the superscript $*$ denotes the complex conjugate, and $e_k(n)$ is given as

$$e_k(n) = \tilde{b}_k(n) - \text{tr}[\mathbf{W}_k^H(n)\mathbf{R}_k(n)], \quad (13)$$

where

$$\tilde{b}_k(n) = \text{sgn}[\text{Re}[\tilde{b}_k(n)]] + j \text{sgn}[\text{Im}[\tilde{b}_k(n)]]. \quad (14)$$

Here, $\text{sgn}[\cdot]$ is the signum function, $\text{Re}[\cdot]$ is the real part of the complex value, and $\text{Im}[\cdot]$ is the imaginary part of the complex value.

In this paper, the initial value $\mathbf{W}_k(0)$ of the weight matrix $\mathbf{W}_k(n)$ for the k th receiver is chosen to be a set of weights that consists of the corresponding initial hopping pattern $\mathbf{P}_k(0)$ and the zero matrix $\mathbf{0}_{\alpha \times M}$ of size $\alpha \times M$, that is,

$$\mathbf{W}_k(0) = [\mathbf{P}_k^T(0) \mathbf{0}_{\alpha \times M}^T]^T, \quad (15)$$

where the superscript T denotes the transpose of the matrix.

2.4 Feedback

Part of the FIR filter weights of the receiver for the k th signal are fed back to the corresponding transmitter, in which they are used as an updated version of the hopping pattern \mathbf{P}_k . When no delay time and no error for the feedback are assumed, the hopping pattern $\mathbf{P}_k(\lambda)$ updated at $t = \lambda T_f + \Delta_k + \alpha T_c + \tau_{k,1}$ ($\lambda = 1, 2, \dots, N_f$; N_f is the number of feedback iterations, T_f is the feedback time-interval, for which we choose an integer multiple of the symbol duration T_s , and Δ_k is the preassigned offset of the feedback timing ($0 \leq \Delta_k < T_f$)) is represented as

$$\mathbf{P}_k(\lambda) \triangleq \begin{bmatrix} p_{k,1,1}(\lambda) & p_{k,1,2}(\lambda) & \cdots & p_{k,1,M}(\lambda) \\ p_{k,2,1}(\lambda) & p_{k,2,2}(\lambda) & \cdots & p_{k,2,M}(\lambda) \\ \vdots & \vdots & \ddots & \vdots \\ p_{k,L,1}(\lambda) & p_{k,L,2}(\lambda) & \cdots & p_{k,L,M}(\lambda) \end{bmatrix} \quad (16)$$

$$= \begin{bmatrix} w_{k,1,1}(\hat{n}_k) & w_{k,1,2}(\hat{n}_k) & \cdots & w_{k,1,M}(\hat{n}_k) \\ w_{k,2,1}(\hat{n}_k) & w_{k,2,2}(\hat{n}_k) & \cdots & w_{k,2,M}(\hat{n}_k) \\ \vdots & \vdots & \ddots & \vdots \\ w_{k,L,1}(\hat{n}_k) & w_{k,L,2}(\hat{n}_k) & \cdots & w_{k,L,M}(\hat{n}_k) \end{bmatrix}, \quad (17)$$

where $\hat{n}_k \triangleq \lfloor (\lambda T_f + \Delta_k + \alpha T_c + \tau_{k,1}) / T_s \rfloor$, and $\lfloor \cdot \rfloor$ is the largest integer that is less than or equal to the operand.

Equations (16) and (17) intend that the value of each element $p_{k,l,m}$ of the hopping pattern is replaced with the value of each element $w_{k,l,m}$ of part of the FIR filter weights at $t = \lambda T_f + \Delta_k + \alpha T_c + \tau_{k,1}$.

Although the updated hopping pattern is fed back to the corresponding transmitter, as in [11], $\mathbf{P}_k(\lambda)$ is altered to obtain a different hopping pattern $\mathbf{P}'_k(\lambda)$ using the PAR control algorithm described in the following section. Furthermore, when the influence of quantization is considered, $\mathbf{P}'_k(\lambda)$ is again altered to obtain $\mathbf{P}''_k(\lambda)$.

3. PAR Control and Quantization

3.1 Proposed Algorithm for PAR Control

Since the updated hopping pattern $\mathbf{P}_k(\lambda)$ is constructed at the receiver, the receiver can reconstruct the updated hopping pattern to control the PAR of the signature waveform $c_k(t)$ to be a small target value PAR_t of the PAR. In this paper, we define the PAR of the signature waveform $c_k(t)$ as

$$\text{PAR} = \frac{\max_{0 \leq t < T_s} |c_k(t)|^2}{1/T_s \int_0^{T_s} |c_k(t)|^2 dt}. \quad (18)$$

Once a hopping pattern $\mathbf{P}_k(\lambda)$ is given, $c_k(t)$ is readily obtained using (1) and (2).

One of the optimum hopping patterns that minimizes the value of the PAR is a hopping pattern $\mathbf{P}'_k(\lambda)$, each row of which contains only one nonzero element having a constant absolute value. This type of hopping pattern yields a signature waveform, each chip of which consists of a single tone having a constant amplitude level, resulting in a minimum value of PAR of 0 dB, because of its constant modulus. Although such a hopping pattern can easily be constructed, it causes severe MAI, especially in wireless asynchronous and multipath environments.

Although the basic concept underlying the proposed algorithm is to construct such a hopping pattern to control the PAR, the proposed algorithm is an attempt to gradually bring $\mathbf{P}_k(\lambda)$ up to such a hopping pattern without the occurrence of MAI in multipath environments with the help of the feedback mechanism in FC/MH-CDMA. Since all K receivers use the proposed algorithm independently, the proposed algorithm is directly applied for decentralized multiple access where no BS exists.

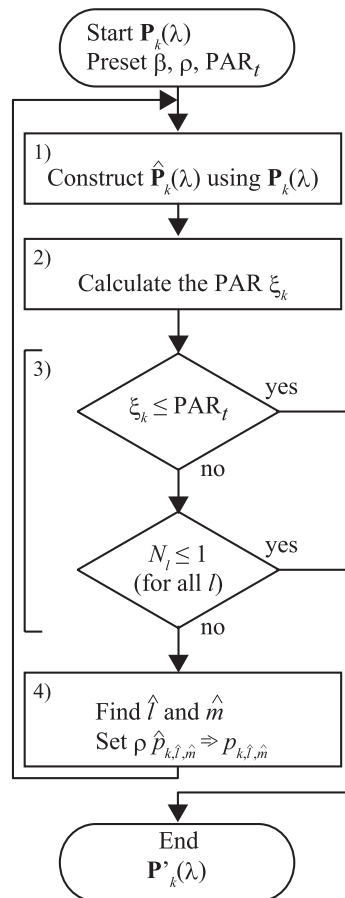


Fig. 3 Flowchart of the PAR control algorithm.

Our algorithm is based on the following considerations. To reduce the value of the PAR of the signature waveform, the chip that has the largest amplitude level must be small. Since FC/MH-CDMA produces a set of signature waveforms, or equivalently, a set of hopping patterns that achieves the highest SINR, the elements (not the chip) that have large amplitudes contained in such a hopping pattern are important for obtaining a high SINR, and conversely, the elements that have small amplitudes are not important for obtaining a high SINR. Therefore, the tone with the smallest amplitude contained in the chip with the largest amplitude can be reduced to obtain a low PAR signal with minimal impact on the SINR. Next, we describe in detail the PAR control algorithm, which is also summarized in Fig. 3. The PAR control algorithm has two design parameters β and ρ in addition to the target value PAR_t of the PAR. Basically, the value of β is chosen to be smaller and ρ is chosen to be greater if a small PAR is required, and vice versa. The impacts of the values of these parameters on the achievable PAR and computational complexity are elaborated through simulations in Sect. 4.2.1.

- 1) Construct an $L \times M$ matrix $\hat{\mathbf{P}}_k(\lambda) = [\hat{p}_{k,l,m}(\lambda)]$ using $\mathbf{P}_k(\lambda)$ such that

$$\hat{p}_{k,l,m} = \begin{cases} 0 & (|p_{k,l,m}| < \gamma) \\ p_{k,l,m} & (|p_{k,l,m}| \geq \gamma) \end{cases}, \quad (19)$$

where γ is the threshold level used to reduce the number of tones and is defined as

$$\gamma = \beta \sqrt{\frac{1}{LM} \|\mathbf{P}_k(\lambda)\|_{\text{F}}^2}, \quad (20)$$

where $\beta (> 0)$ is a positive real constant that represents the threshold level normalized to the root mean squared value $\sqrt{\frac{1}{LM} \|\mathbf{P}_k(\lambda)\|_{\text{F}}^2}$ of the elements of $\mathbf{P}_k(\lambda)$. We assume that N_l ($0 \leq N_l \leq M$, $l = 1, 2, \dots, L$) is the number of nonzero elements contained in the l th row of the matrix $\hat{\mathbf{P}}_k(\lambda)$.

- 2) Calculate the value ξ_k of the PAR for the signature waveform $\hat{c}_k(t)$ obtained using the matrix $\hat{\mathbf{P}}_k(\lambda)$ and compare ξ_k with the target value PAR_t of the PAR.
- 3) If $\xi_k \leq \text{PAR}_t$, or if $N_l \leq 1$ for all l , then the matrix $\hat{\mathbf{P}}_k(\lambda)$ can be used as $\mathbf{P}'_k(\lambda)$ for the feedback to the transmitter.
- 4) If $\xi_k > \text{PAR}_t$, and if $N_l > 1$ for one of the L values of N_l , then find a chip index \hat{l} ($1 \leq \hat{l} \leq L$), which indicates that the \hat{l} th chip has the largest value of absolute amplitude $|\hat{c}_k(t)|$, and find a tone index \hat{m} ($1 \leq \hat{m} \leq M$), which indicates that the absolute value $|\hat{p}_{k,\hat{l},\hat{m}}(\lambda)|$ of the \hat{m} th tone in the \hat{l} th chip is the smallest nonzero value, and then change the value of $p_{k,\hat{l},\hat{m}}(\lambda)$ to a smaller value $\rho \cdot \hat{p}_{k,\hat{l},\hat{m}}(\lambda)$ by a factor of ρ ($0 < \rho < 1$), where the factor ρ corresponds to the sensitivity for reducing the value of the PAR increased by the (\hat{l}, \hat{m}) th entry of $\mathbf{P}_k(\lambda)$.

Steps 1) through 4) are repeated until the condition given in Step 3) is satisfied.

Basically, FC/MH-CDMA finds a hopping pattern $\mathbf{P}_k(\lambda = \lambda_0)$ that achieves a smaller BER, and the hopping pattern $\mathbf{P}_k(\lambda_0)$ is modified to $\mathbf{P}'_k(\lambda_0)$ by the proposed algorithm, which achieves the target value PAR_t of the PAR at the cost of increasing the BER. However, $\mathbf{P}'_k(\lambda_0)$ is fed back to the transmitter at the $\lambda = \lambda_0$ th round of feedback, and $\mathbf{P}'_k(\lambda_0)$ is modified to $\mathbf{P}_k(\lambda_0 + 1)$, which achieves a smaller BER at the cost of increasing the PAR, at the receiver in FC/MH-CDMA. $\mathbf{P}_k(\lambda_0 + 1)$ is modified to $\mathbf{P}'_k(\lambda_0 + 1)$ by the proposed algorithm, which achieves the target value PAR_t at the cost of increasing the BER and is fed back again to the transmitter. By repeating the above process, the proposed algorithm controls the PAR to a preset target value while retaining good BER performance in FC/MH-CDMA.

3.2 Quantization

In order to reduce the amount of feedback information on the hopping pattern $\mathbf{P}'_k(\lambda)$, we discuss the required number of quantization bits.

Let $a_k^{\max}(\lambda)$ be the maximum absolute value of the real and imaginary parts in all elements of the hopping pattern $\mathbf{P}'_k(\lambda) = [p'_{k,l,m}]$ obtained using the PAR control algorithm, that is,

$$a_k^{\max}(\lambda) = \max_{l,m} [|\text{Re}[p'_{k,l,m}(\lambda)]|, |\text{Im}[p'_{k,l,m}(\lambda)]|]. \quad (21)$$

The elements $p''_{k,l,m}(\lambda)$ of a quantized hopping pattern $\mathbf{P}''_k(\lambda) = [p''_{k,l,m}(\lambda)]$ are given by

$$p''_{k,l,m}(\lambda) = \frac{a_k^{\max}(\lambda)}{2^{q-1}} \left[\frac{p'_{k,l,m} 2^{q-1}}{a_k^{\max}(\lambda)} \right]_{\text{round}}, \quad (22)$$

where $[\cdot]_{\text{round}}$ denotes rounding to the nearest integer of the operand, and $(q+1)$ is the number of bits required to quantize each of the real and imaginary parts in all elements of $\mathbf{P}'_k(\lambda)$. This is referred to as midtread-type uniform quantization. Therefore, $2(q+1)LM$ bits are required for the feedback for each quantized hopping pattern.

4. Performance Evaluation

4.1 Specifications

4.1.1 Multipath Model

We assume a six-path model (i.e., $I_k = 6$ for all k) that has a delay profile of exponential decay, where the relative intensities of $|h_{k,i}|$ are $20 \log_{10}(|h_{k,i+1}|/|h_{k,i}|) = -3$ dB ($i = 1, 2, \dots, I_k - 1$), the path delays $\tau_{k,i}$ are $\tau_{k,i+1} - \tau_{k,i} = \frac{L+1}{16} T_c$ ($\approx \frac{1}{16} T_s$ for $L = 7$), and $\tau_{k,1}$ and $\theta_{k,i}$ (for all k and i) are mutually statistically independent, uniformly distributed random variables in the intervals of $[0, T_s)$ and $[0, 2\pi)$, respectively.

In addition to this exponential delay profile, we also employ a six-path uniform delay profile ($20 \log_{10}(|h_{k,i+1}|/|h_{k,i}|) = 0$ dB ($i = 1, 2, \dots, I_k - 1$)) only in Sect. 4.2.3.

4.1.2 Other Specifications

FC/MH-CDMA requires an initial training period during which the receiver returns part of the filter weights, $\mathbf{P}_k(\lambda)$, or its altered version, $\mathbf{P}'_k(\lambda)$ or $\mathbf{P}''_k(\lambda)$, to the corresponding transmitter. In this paper, we define the initial training period as $t < (N_f + 1)T_f + \Delta_k + \tau_{k,1}$ and discuss the BER performance in the steady period, which is defined as the period after the initial training period, that is, $t \geq (N_f + 1)T_f + \Delta_k + \tau_{k,1}$. In the initial training period, the PAR control algorithm and quantization are applied to $\mathbf{P}_k(\lambda)$ just prior to when the receiver returns the hopping pattern to the transmitter. In the steady period, only the filter weights are updated at the receiver (i.e., no feedback). We assume that the reference $\hat{b}_k(n)$ used for updating the filter weights is $\hat{b}_k(n) = b_k(n)$ during the initial training period, which implies that the receiver has prior knowledge of the pilot data symbols used for the initial training. Since both the BER and the PAR depend slightly on the randomly chosen values of $\tau_{k,1}$ and $\theta_{k,i}$, all of the plots are of the average of ten simulation trials. Other common specifications are listed in Table 1.

4.2 Simulation Results

4.2.1 Parameter Settings

First we discuss the convergence characteristic of the weight

Table 1 Common specifications.

	FC/MH-CDMA	DS-CDMA	
Message symbol		QPSK	
E_b/N_0		9.6 dB	
Spreading	Eq. (4)	2D block spreading [16]	Ordinary DS
Initial code	Random patterns $\{+1, -1\}$	Hadamard code $\{+1, -1\}$	Random code $\{+1, -1\}$
Scrambling code	-	Random code $\{+1, -1\}$	-
L	7	32, 64 (SF^c, SF^b) = (32/ K or 64/ K , K)	32, 64
α	7	-	-
M	8	-	-
Samples per chip	8	1	-
T_f	$10^4 T_s$	-	-
N_f	10	-	-
Δ_k	Uniform distribution in $[0, T_f)$	-	-
GI	-	Cyclic prefix ($N_g = 16$)	-
Receiver	Adaptive filter (N-LMS ($\mu = 0.1$))	Ideal MMSE-FDE ($N_c = 256$)	RAKE (Ideal six-finger MRC) MF
Transmit timing control	No (Asynchronous)	Yes (Synchronous)	No (Asynchronous)

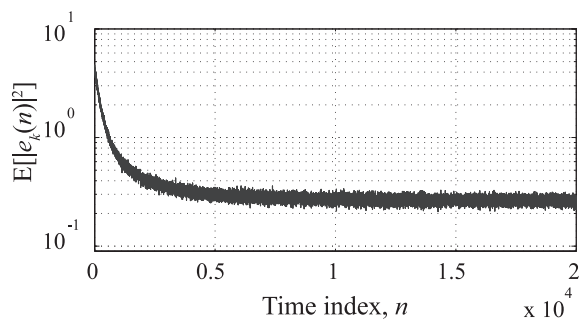


Fig. 4 Ensemble average of squared error $|e_k(n)|^2$ ($K = 32$ and $\mu = 0.1$).

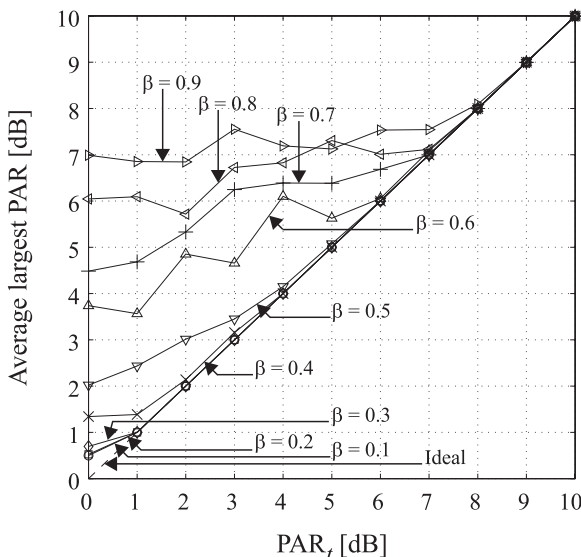


Fig. 5 PAR vs. β ($\rho = 0.9$ and $K = 32$).

matrix (11) updated by the N-LMS algorithm using the step size parameter $\mu = 0.1$ listed in Table 1. Figure 4 shows the characteristic of the ensemble average $E[|e_k(n)|^2]$ of the

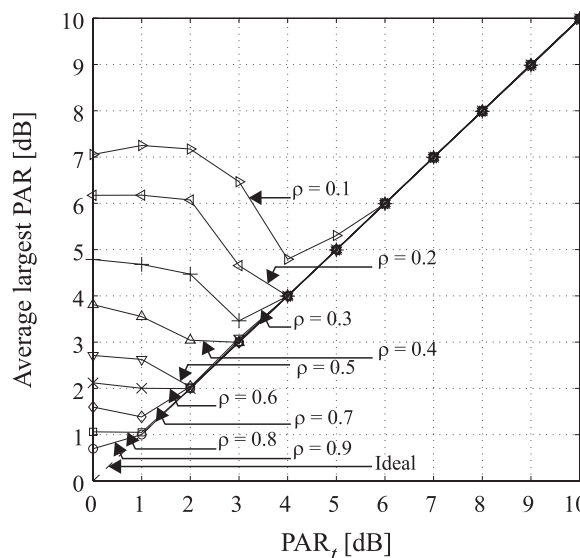
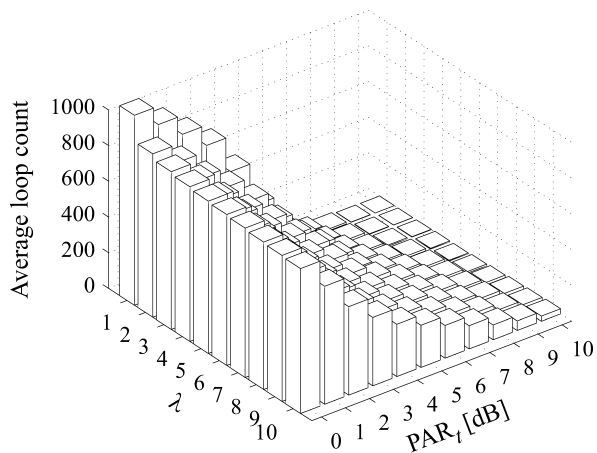


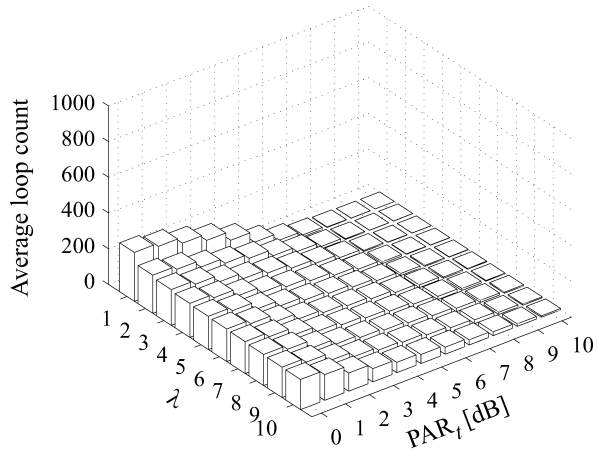
Fig. 6 PAR vs. ρ ($\beta = 0.3$ and $K = 32$).

squared error $|e_k(n)|^2$ vs the time index n of the symbol interval T_s , where the number of active signals, K , was chosen to be 32. It is observed from Fig. 4 that 10^4 iterations are sufficient for the adaptation of the weight matrix when $\mu = 0.1$. Therefore, we choose the value of T_f to be $10^4 T_s$, during which the N-LMS adaptation can be sufficiently accomplished and the receiver can be made ready for the feedback.

Next, the proposed PAR control algorithm is verified to effectively control the PAR of the signature waveform $c_k(t)$. Since the PAR control algorithm has two design parameters β and ρ in addition to the target value PAR_t , we first set these parameters appropriately. Again, since the PAR control algorithm repeats Steps 1) through 4), as shown in Fig. 3, we also investigate the computational complexity in



(a) $\beta = 0.1$ and $\rho = 0.9$



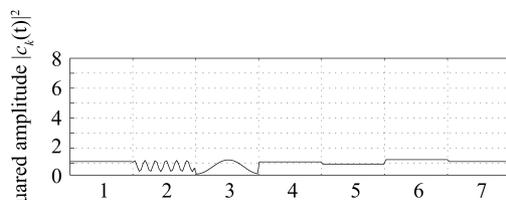
(b) $\beta = 0.3$ and $\rho = 0.8$

Fig. 7 Average loop count for the PAR control algorithm required to reconstruct $\mathbf{P}'_k(\lambda)$ from $\mathbf{P}_k(\lambda)$ obtained at $t = \lambda T_f + \Delta_k + \alpha T_c + \tau_{k,1}$ ($K = 32$).

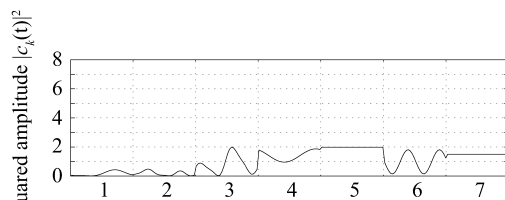
terms of the average loop count of Steps 1) through 4) from the start to the end of the algorithm executed to reconstruct $\mathbf{P}'_k(\lambda)$ from $\mathbf{P}_k(\lambda)$ for each λ th round of feedback.

Figure 5 shows the characteristic of PAR vs. PAR_t for different values of β , where K was chosen to be 32. Note that, in Fig. 5, the term average largest PAR denotes the largest value of the PAR among the K ($= 32$) waveforms $c_k(t)$ using $\mathbf{P}'_k(\lambda = 10)$, averaged by ten simulations, obtained after the initial training period. The factor ρ was chosen to be 0.9. Figure 5 shows that if $\beta \leq 0.3$, then the values of the PAR obtained are widely fit to the preset values of the target PAR except for $\text{PAR}_t < 1$ dB.

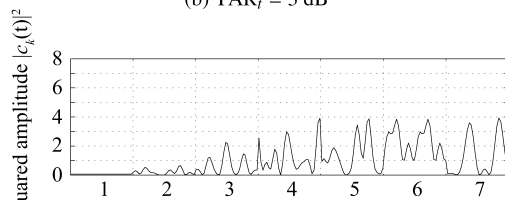
Figure 6 shows the characteristics of the average largest PAR vs. PAR_t for different values of ρ with normalized threshold $\beta = 0.3$ and $K = 32$. Figure 6 indicates that if $\rho \geq 0.8$, then the average largest PAR coincides with the preset value of the target PAR, except for $\text{PAR}_t < 1$ dB. It is



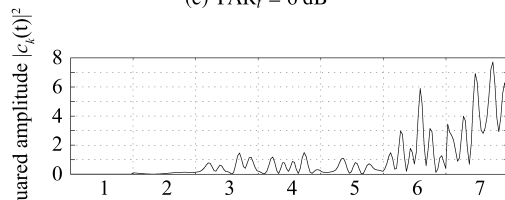
(a) $\text{PAR}_t = 1$ dB



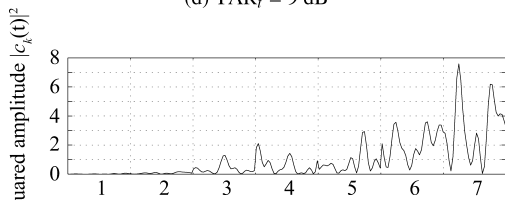
(b) $\text{PAR}_t = 3$ dB



(c) $\text{PAR}_t = 6$ dB



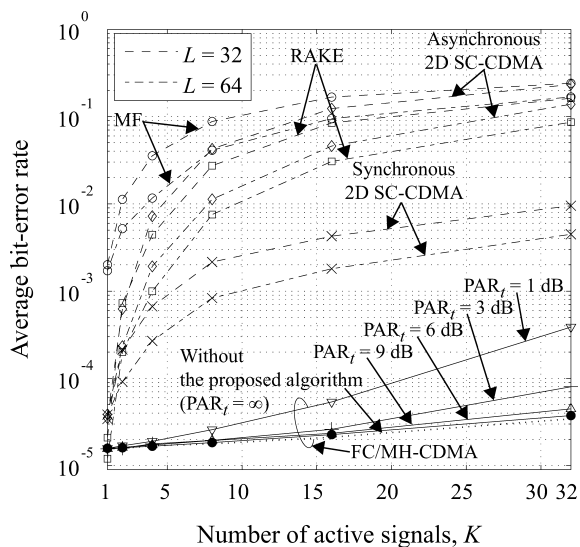
(d) $\text{PAR}_t = 9$ dB



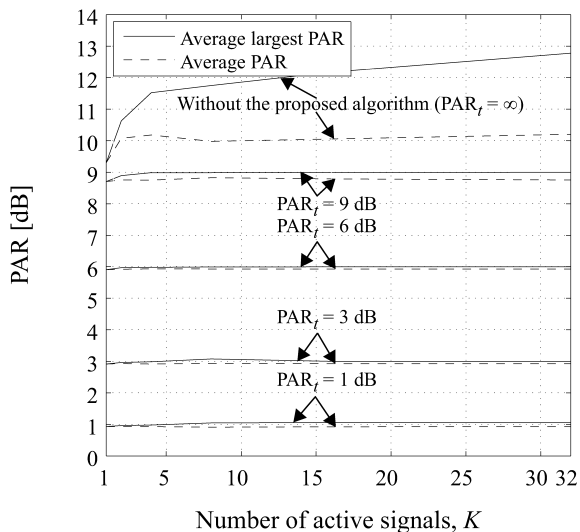
(e) Without PAR control ($\text{PAR}_t = \infty$)

Fig. 8 Examples of signature waveforms for $\overline{|c_k(t)|^2} = 1$ ($\beta = 0.3$, $\rho = 0.8$, and $K = 32$).

observed from Fig. 6 that the average largest PAR increases with decreasing PAR_t for small values of ρ such as $\rho = 0.1$. For small values of PAR_t , the PAR control algorithm is completed for most cases when the condition “ $N_l \leq 1$ for all l ” in Step 3) has been satisfied. Since this condition is rapidly satisfied through the coarse operation in Step 4) when the value of ρ is small, the resultant value of the PAR becomes large for small values of PAR_t in the case of a small value of ρ . Note that for a certain desired value of the PAR, the



(a) BER



(b) PAR

Fig. 9 Effect of multiple access ($\beta = 0.3$ and $\rho = 0.8$).

computational complexity required to produce the hopping pattern $\mathbf{P}'_k(\lambda)$ from $\mathbf{P}_k(\lambda)$ by the proposed algorithm can be reduced by appropriately choosing the values of β and ρ . Figures 7(a) and 7(b) show the histograms of the average loop count for the different parameter settings $\{\beta, \rho\} = \{0.1, 0.9\}$ and $\{0.3, 0.8\}$, where the average largest PAR of 1 dB is achievable for both settings. Figures 7(a) and 7(b) indicate that the average loop count is greatly reduced by selecting appropriate values of β and ρ . To reduce the average loop count, the value of β is chosen to be greater and ρ is chosen to be smaller if the required PAR is achievable. In the following, since we discuss a wide range of the target PAR, we select the set of values of $\{\beta, \rho\} = \{0.3, 0.8\}$.

The signature waveforms $c_k(t)$ using $\mathbf{P}'_k(\lambda = 10)$ obtained for $K = 32$ in several cases of the target PAR are shown in Figs. 8(a) through 8(e), where all the squared am-

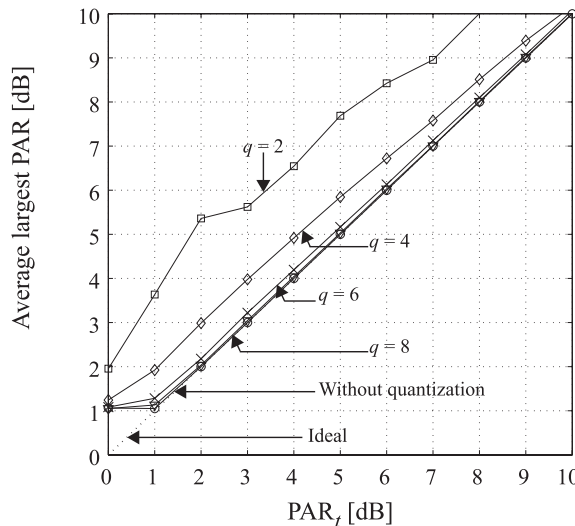
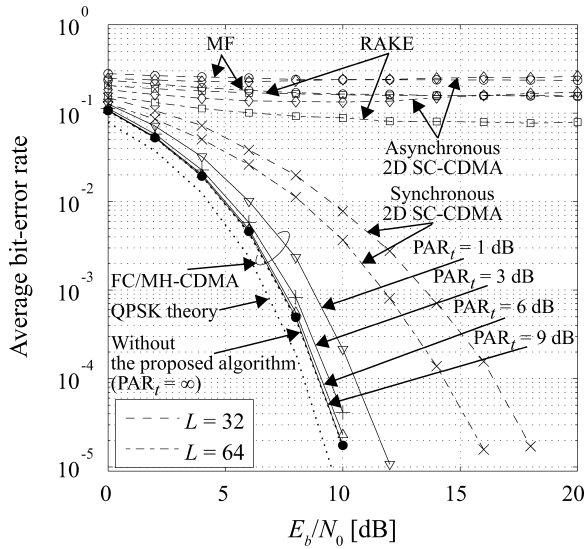


Fig. 10 PAR vs. the number of quantization bits ($\beta = 0.3, \rho = 0.8$, and $K = 32$).

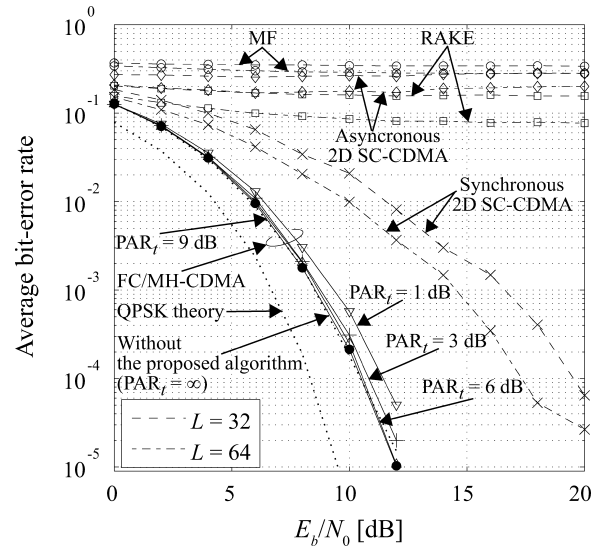
plitudes of $c_k(t)$ have a unit mean value. The fluctuation of the squared amplitude $|c_k(t)|^2$ depends on the value of PAR_t . For larger values of PAR_t , the signature waveform $c_k(t)$ has very small amplitudes in the few first chips and large amplitudes in the remaining chips. This means that FC/MH-CDMA embeds the so-called zero-padding guard interval in the signature waveform to combat ISI caused by the channel multipath. On the other hand, for $\text{PAR}_t = 1$ dB, the signal energy is uniformly distributed in all of the chips to achieve a small value of the PAR.

4.2.2 BER Performance

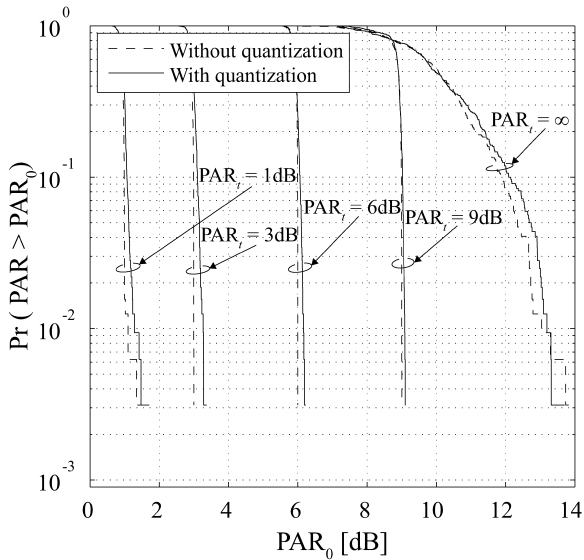
The BER performance of FC/MH-CDMA using the PAR control algorithm is shown in Fig. 9(a), where the BER performance of DS-CDMA using random sequences with the matched filter (MF) with/without the RAKE combining method (six-finger maximal ratio combining (MRC)), and the BER performance of the block transmission of DS-CDMA using two-dimensional spreading and MMSE-FDE (2D SC-CDMA) [16] are also shown for reference. For the comparison of performance, we consider $L = 32$ and 64 for all cases of DS-CDMA, as listed in Table 1. When a rectangular pulse is assumed as the elementary pulse shape for DS-CDMA as in the case of FC/MH-CDMA ($g(t)$ in (2)), the bandwidth (null-to-null bandwidth criterion) of DS-CDMA with $L = 32$ is almost identical to that of FC/MH-CDMA at a common transmission rate. In this case, the value of the PAR, defined by (18), for DS-CDMA will be 0 dB if QPSK symbols are assumed to be transmitted. Another type of elementary pulse shape is obtained using the root-raised cosine filter, which occupies a narrower bandwidth than that of the rectangular pulse at a common transmission rate. When the roll-off factor is chosen to be zero, the pulses are most spectrally efficient and DS-CDMA with $L = 64$ using such a pulse occupies an almost identical bandwidth to that of



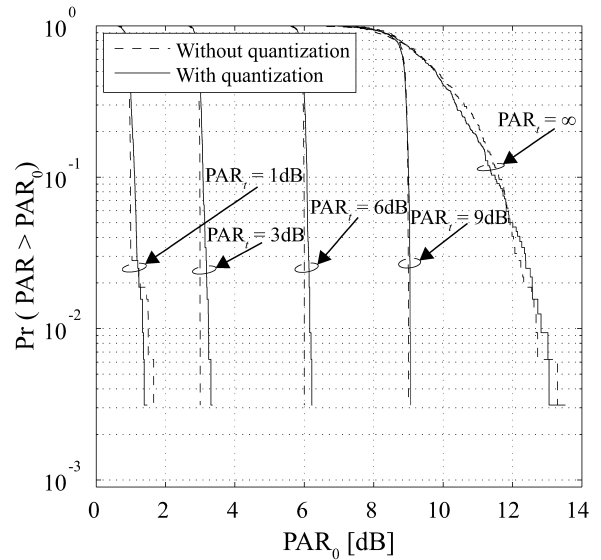
(a) BER characteristics



(a) BER characteristics



(b) CCDFs



(b) CCDFs

Fig. 11 BER characteristics and CCDFs of PAR for the case in which an exponential delay profile is assumed ($\beta = 0.3$, $\rho = 0.8$, $K = 32$, and $q = 6$ bits).

Fig. 12 BER characteristics and CCDFs of PAR for the case in which a uniform delay profile is assumed ($\beta = 0.3$, $\rho = 0.8$, $K = 32$, and $q = 6$ bits).

FC/MH-CDMA at a common transmission rate. It is known that the value of the PAR of single-carrier QPSK transmission using the root-raised-cosine-filtered pulses is 3 dB or more for a roll-off factor greater than around 0.4, and is 6 dB or more for a roll-off factor of zero [17]. Since 2D SC-CDMA requires a CP-GI, which lengthens the duration of the transmitted signal, its transmission rate becomes slightly low.

Figure 9(a) indicates that when the number of active signals, K , is large, the proposed PAR control algorithm slightly deteriorates the BER of FC/MH-CDMA if $PAR_t = 1$ dB or 3 dB. On the other hand, if $PAR_t = 6$ dB or 9 dB, the BER is almost identical to that without the proposed PAR

control. Figure 9(b) shows the characteristics of both the average largest PAR and the average PAR as functions of K . Figure 9(b) indicates that the PAR control algorithm works well independent of K .

4.2.3 Effect of Quantization

We investigate the relationship between the PAR and q (the number of quantizing bits per real or imaginary part per chip per frequency). Here, we assume the midtread-type uniform quantization described in Sect. 3.2.

Figure 10 shows the average largest PAR vs. PAR_t for $K = 32$. The figure shows that the PAR performance for the case in which $q \geq 6$ is almost identical to that for the case

with no quantization.

The characteristics of the BER vs. E_b/N_0 for $K = 32$ and $q = 6$ bits are shown in Fig. 11(a), and the complementary cumulative distribution functions (CCDFs), $\Pr(\text{PAR} > \text{PAR}_0)$, of the PAR for $\mathbf{P}'_k(\lambda = 10)$ (without quantization) and $\mathbf{P}''_k(\lambda = 10)$ (with quantization) using 320 hopping patterns obtained through ten simulation trials for $K = 32$, $q = 6$ bits, and $E_b/N_0 = 9.6$ dB are shown in Fig. 11(b). Figure 11(a) indicates that the proposed algorithm achieves sufficient BER performance even when $\text{PAR}_t = 1$ dB or 3 dB. Again, Fig. 11(b) indicates that the PAR becomes slightly large with quantization for the hopping patterns.

So far we have considered a six-path channel model that has an exponential delay profile. Finally, we consider a six-path channel model that has a uniform delay profile. Figures 12(a) and 12(b) show the characteristics of the BER vs. E_b/N_0 , and the CCDFs, in which the same parameters as those in Figs. 11(a) and 11(b) are chosen, except that a uniform delay profile is assumed. The curves for FC/MH-CDMA shown in Fig. 12(a) are shifted to the right by 1.6 dB at a BER of 10^{-4} in comparison with those shown in Fig. 11(a) because of the large delay spread of the channel. It is observed from Fig. 12(a) that the proposed PAR control algorithm only slightly deteriorates the BER of FC/MH-CDMA independent of the channel delay profile. It is also verified from Fig. 12(b) that CCDF characteristics similar to those shown in Fig. 11(b) are obtained independent of the channel delay profile.

Note that the asynchronous multiple-access performance is considered in multipath environments for all of the results except for the case in which synchronous 2D SC-CDMA is considered.

5. Conclusion

A PAR control algorithm for asynchronous FC/MH-CDMA signals was proposed, and the relationship between the PAR and the BER was shown over a time-invariant multipath channel. The effect of the quantization was investigated, and it was demonstrated that time-frequency hopping patterns that achieve small values of the target PAR can be constructed using the proposed algorithm. The BER was also shown to have little effect if the target PAR is larger than 3 dB.

The proposed PAR control algorithm is directly applicable to autonomous, decentralized, multiple-access systems.

References

- [1] J.G. Proakis, *Digital Communications*, 3rd ed., McGraw-Hill, New York, 1995.
- [2] W.C. Jakes, *Microwave Mobile Communications*, IEEE Press, New Jersey, 1974.
- [3] T.S. Rappaport, *Wireless Communications*, 2nd ed., Prentice Hall, New Jersey, 2002.
- [4] G. Marubayashi, M. Nakagawa, and R. Kohno, *Spread Spectrum Communications and Its Applications*, IEICE, Tokyo, 1998.
- [5] D.J. Love, R.W. Heath, Jr., V.K.N. Lau, D. Gesbert, B.D. Rao, and M. Andrews, "An overview of limited feedback in wireless communication systems," *IEEE J. Sel. Areas Commun.*, vol.26, no.8, pp.1341–1365, Oct. 2008.
- [6] S. Hamada, M. Hamamura, H. Suzuki, and S. Tachikawa, "A proposed DS/CDMA system using analog PN sequences produced by adaptive filters," *IEICE Trans. Fundamentals*, vol.E81-A, no.11, pp.2261–2268, Nov. 1998.
- [7] S. Ulukus and R.D. Yates, "Iterative constructions of optimum signature sequence sets in synchronous CDMA systems," *IEEE Trans. Inf. Theory*, vol.47, no.5, pp.1989–1998, July 2001.
- [8] L.R. Welch, "Lower bounds on the maximum cross correlation of signals," *IEEE Trans. Inf. Theory*, vol.20, no.3, pp.397–399, May 1994.
- [9] M. Rupp and J.L. Massey, "Optimum sequence multisets for synchronous code-division multiple-access channels," *IEEE Trans. Inf. Theory*, vol.40, no.4, pp.1261–1266, July 1994.
- [10] T. Miyatake, K. Chiba, M. Hamamura, and S. Tachikawa, "Asynchronous, decentralized DS-CDMA using feedback-controlled spreading sequences for time-dispersive channels," *IEICE Trans. Commun.*, vol.E91-B, no.1, pp.53–61, Jan. 2008.
- [11] K. Chiba and M. Hamamura, "Multitone-hopping CDMA using feedback-controlled hopping pattern for decentralized multiple access," *IEICE Trans. Fundamentals*, vol.E91-A, no.12, pp.3723–3730, Dec. 2008.
- [12] X. Li and L.J. Cimini, Jr., "Effects of clipping and filtering on the performance of OFDM," *IEEE Commun. Lett.*, vol.2, no.5, pp.131–133, May 1998.
- [13] R.W. Bauml, R.F.H. Fischer, and J.B. Huber, "Reducing the peak-to-average power ratio of multicarrier modulation by selected mapping," *Electron. Lett.*, vol.32, no.22, pp.2056–2057, Oct. 1996.
- [14] B.M. Popovic, "Synthesis of power efficient multitone signals with flat amplitude spectrum," *IEEE Trans. Commun.*, vol.39, no.7, pp.1031–1033, July 1991.
- [15] H. Ochiai and H. Imai, "Block coding scheme based on complementary sequences for multicarrier signals," *IEICE Trans. Fundamentals*, vol.E80-A, no.11, pp.2136–2143, Nov. 1997.
- [16] F. Adachi, H. Tomeba, and K. Takeda, "Frequency-domain equalization for broadband single-carrier multiple access," *IEICE Trans. Commun.*, vol.E92-B, no.5, pp.1441–1456, May 2009.
- [17] S. Daumont, B. Rihawi, and Y. Lout, "Root-raised cosine filter influences on PAPR distribution of single carrier signals," *IEEE ISCCSP 2008*, pp.841–845, March 2008.
- [18] K. Chiba and M. Hamamura, "Peak-to-average-power ratio of multitone-hopping CDMA signals using feedback-controlled hopping patterns," *Proc. WINSYS2008*, pp.145–150, Porto, July 2008.
- [19] S. Haykin, *Adaptive Filter Theory*, 3rd ed., Prentice Hall, New Jersey, 1996.



Kazuki Chiba received the B.E. degree in Information Systems Engineering from Kochi University of Technology, Kochi, Japan, in 2008. He is currently working toward the M.E. degree in Information Systems Engineering at Kochi University of Technology, Kochi, Japan. His research interests lie in the area of feedback-based communication systems.



Masanori Hamamura received his B.S., M.S. and Ph.D. degrees in electrical engineering from Nagaoka University of Technology, Nagaoka, Japan, in 1993, 1995 and 1998, respectively. From 1998 to 2000, he was a Research Fellow of the Japan Society for the Promotion of Science. Since 2000, he has been with the Department of Information Systems Engineering at Kochi University of Technology, Kochi, Japan, where he is now an Associate Professor. From 1998 to 1999, he was a visiting researcher at

Centre for Telecommunications Research, King's College London, United Kingdom, where he worked on adaptive signal processing for mobile systems. His current research interests are in the areas of spread spectrum systems, wireless communications and signal processing. Dr. Hamamura is a member of IEEE and SITA of Japan.